J Mater Sci (2008) 43:3560–3568
DOI 10.1007/s10853-008-2562-9

# Effect of piezoelectric grain size on magnetoelectric coefficient of $Pb(Zr_{0.52}Ti_{0.48})O_3$–$Ni_{0.8}Zn_{0.2}Fe_2O_4$ particulate composites

**Rashed Adnan Islam · Shashank Priya**

Received: 14 December 2007 / Accepted: 14 February 2008 / Published online: 23 March 2008


**Abstract** This study investigates the variation of magnetoelectric (ME) coefficient as a function of the piezoelectric grain size in the composite system of 0.8 $Pb(Zr_{0.52}Ti_{0.48})O_3$–0.2 $Ni_{0.8}Zn_{0.2}Fe_2O_4$. It was found that as the piezoelectric-phase grain size increases the overall resistivity, piezoelectric, dielectric, and ferroelectric property of the composite increases and saturates above 600 nm. Below 200 nm average grain size, piezoelectric and dielectric properties decrease rapidly. The ferroelectric Curie temperature was found to decrease from 377 to 356 °C as the average grain size decreases from 830 to 111 nm. ME coefficient of the composite showed a rapid change below grain size of 200 nm and was found to saturate above 600 nm to a value of 155 mV/cm.Oe.

## Introduction

Magnetoelectric (ME) effect in particulate sintered composites has been obtained by combining magnetostrictive and piezoelectric phases [1–5]. Sintered composites consisting of piezoelectric phases, $Pb(Zr, Ti)O_3$ and $BaTiO_3$, and ferromagnetic phases, $CoFe_2O_4$, $NiFe_2O_4$, $LiFe_5O_8$, and $CuFe_2O_4$, have been widely studied because of simplicity in synthesis using conventional ceramic processing [6–11]. Composition, microstructure, and geometry play important role on the magnitude of the ME coefficient. The effect of composition variation has been investigated by doping the PZT and ferrites, and utilizing relaxor-based compositions. The effect of geometry has also been investigated by synthesizing bilayers, sandwich structures, 2-1 composites, and 2-2 composites. However, the effect of microstructure has not been studied in detail. The pioneering studies at Phillips Laboratories showed that texturing improves the ME coefficient by providing higher piezoelectric coefficients. In this study, we elucidate the effect of piezoelectric grain size on the magnitude of ME coefficient. We select the model system, 0.8 $Pb(Zr_{0.52}Ti_{0.48})O_3$–0.2 $Ni_{0.8}Zn_{0.2}Fe_2O_4$ [PZT–20 NZF], for this study.

Effect of grain size on piezoelectric, dielectric, and ferroelectric properties has been widely studied in literature [12–16]. It is well known that piezoelectric, and dielectric properties drop rapidly below critical grain size ($\sim$100 nm) [17, 18]. SEM analysis combined with the surface tension measurement indicate that the surface bond contraction due to small size induces a compressive stress on the inner part of a grain and this effect plays an important role in ferroelectric materials in the nanometer size range. The induced stress causes decrease of Curie temperature and spontaneous polarization with decreasing grain size. The domain wall contribution has an opposite effect as compared with the surface bond contraction induced effect. When the grain size decreases to a value comparable to the width of domain walls, pinning points develop inside the grains and the domain wall motion is inhibited. The reduced wall mobility causes a decrease in the relative permittivity. The measured value is a competition between the increase of relative permittivity by the surface bond contraction effect and its decrease by the domain wall pinning effect [19–22].

R. A. Islam
Materials Science and Engineering, University of Texas at Arlington, Arlington, TX 76019, USA

S. Priya (✉)
Materials Science and Engineering, Virginia Tech, Blacksburg, VA 24061, USA
e-mail: spriya@vt.edu

## Experimental

Reagent-grade powders of PbO, $ZrO_2$, $TiO_2$, NiO, ZnO, and $Fe_2O_3$ were obtained from Alfa Aesar, MA. Stoichiometric ratios of the powders were mixed according to compositions $Pb(Zr_{0.52}Ti_{0.48})O_3$ (PZT), and $Ni_{0.8}Zn_{0.2}Fe_2O_4$ (NZF), and ball milled separately for 24 h with alcohol and YSZ grinding media (5 mm diameter, Tosoh Co. Tokyo, Japan). After drying at 80 °C, PZT powders were calcined at 750 °C for 2 h and ferrite powders (NZF) were calcined at 1,000 °C for 5 h in separate alumina crucibles. The calcined powders were crushed, sieved, and observed using X-ray Diffraction (XRD, Siemens Krystalloflex 810 D500) for formation of single phase (perovskite for PZT and spinel for NZF). About 20 mole percent of calcined ferrite powders was mixed with PZT powders in alcohol and ball milled for 24 h. The slurries were dried at 80 °C and crushed. Small amount of powders (10 gm) was taken in stainless steel vial and mixed with alcohol and YSZ grinding media (3, 5, or 10 mm) and milled in high-energy 3-D planetary milling machine (Spex 8000 M mixer mill) for 3–15 h. The slurries were again dried at 80 °C, crushed and sieved with a stainless steel sieve of US mesh #170. The powders were than pressed to pellets of size $12.7 \times 1.5$ mm$^2$ in a hardened steel die using hydraulic press under a pressure of 15 MPa. The pellets were sealed in a vacuum bag and pressed isostatically in a cold isostatic press (CIP) under a pressure of 310 MPa. Pressureless sintering of composites was performed in air using a Lindberg BlueM furnace in the range of 1,050–1,150 °C for 2–5 h.

The density of samples was measured by Archimedes principle. Microstructural analysis was done by Zeiss Leo Smart SEM using the polished and thermally etched sintered samples. Grain size was measured using linear intercept method. In order to perform piezoelectric measurements, an Ag/Pd electrode was applied on the samples and fired at 850 °C for 1 h. The specimens were poled under a D.C. field of 2.5 kV/mm for 20 min. in a silicone oil bath at 120 °C. The piezoelectric constant was measured by APC YE 2730A $d_{33}$ meter. Resonance characteristics were determined by HP 4194A impedance analyzer (Hewlett Packard Co. USA). Dielectric constant as a function of temperature was measured via HP 4274A LCR meter (Hewlett Packard Co. USA). Resistivity and the polarization-electric field loop was measured using Precision LC (Radiant Technologies Inc., USA) with an external amplifier of 2 kV. The magnetic properties of the sintered samples were measured at room temperature by using alternating gradient force magnetometer (AGFM).

Magnetoelectric coefficient (dE/dH) was measured by applying an A.C. magnetic field at 1 kHz and 1Oe amplitude (H) under varying DC magnetic bias. The AC magnetic field was generated by a Helmholtz coil powered by Agilent 3320 function generator. The output voltage generated from the composite was measured using a SRS DSP lock-in amplifier (model SR 830).

## Results and discussions

Figure 1a shows the XRD patterns of starting powder as a function of final grain size. No secondary peaks were found other than perovskite (P) and spinel (S). As the grain size decreases the intensity of the peaks also decreases. Another important feature that can be noted is that with decreasing grain size the peak width increases. The full width half maximum (FWHM) was quantified from the XRD pattern and is plotted as a function of grain size in Fig. 1b. The 101/110 peaks were chosen for the FWHM measurement, shown by a set of arrows in Fig. 1a. For a final grain size of 97 nm the FWHM for 101/110 peak was recorded as

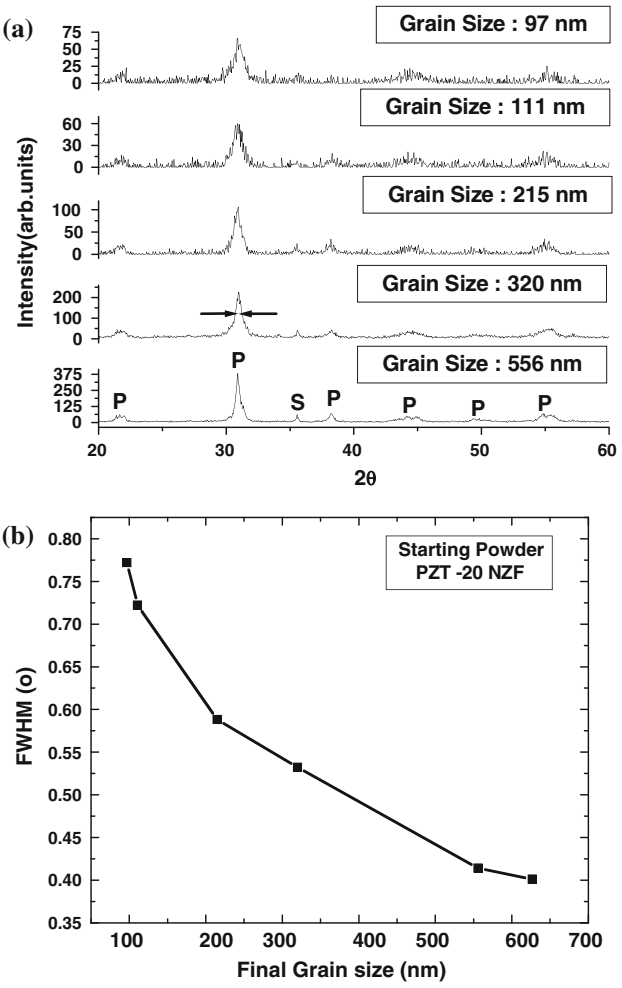


**Fig. 1** Structural characterization of calcined powder (**a**) XRD patterns of composite powders and (**b**) Full width half maxima (FWHM) as a function of final grain size in sintered sample

0.772°, whereas the FWHM for the 627 nm grain size was found to be as 0.401°. Figure 2 shows the histogram patterns of particle size distribution of four different batches of powders. It was found that the starting average particles size of 76 nm produces a final grain size of 97 nm, whereas the average particle size of 486 nm produces ~556 nm grain size. Grain growth in the range of 15–25% was observed during sintering.

Figure 3a–f shows the SEM microstructure of ME composite with 830, 758, 556, 320, 111, and 97 nm average piezoelectric grain size, respectively. In this article only the effect of piezoelectric grainsize was considered. All the microstructures were found to be dense and well sintered. The density data shown in Fig. 4a illustrates that as the grain size of the composite decreases the density increases and at grain size of 97 nm the densification

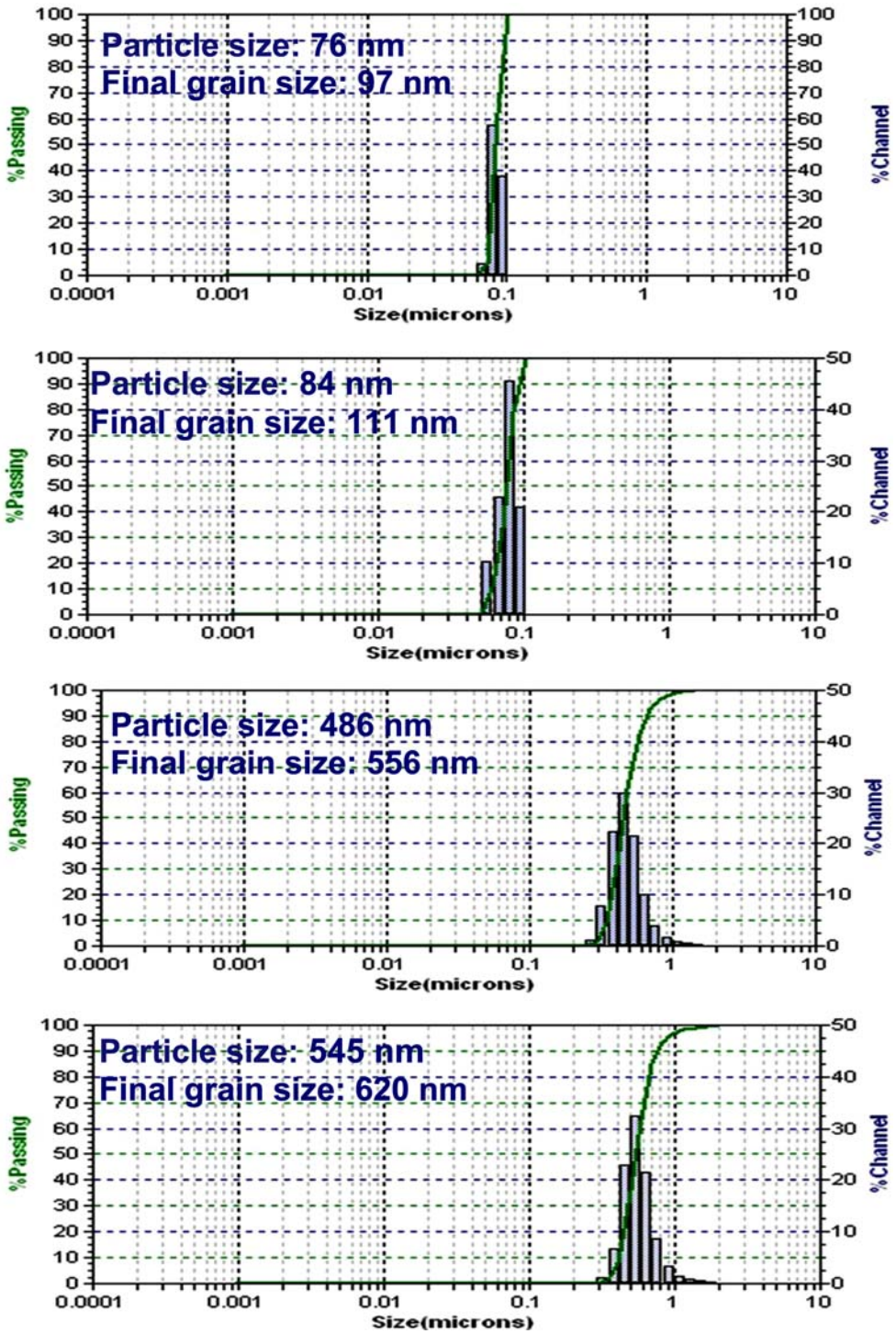


**Fig. 2** Initial particle size distribution histogram for four different batches of powders

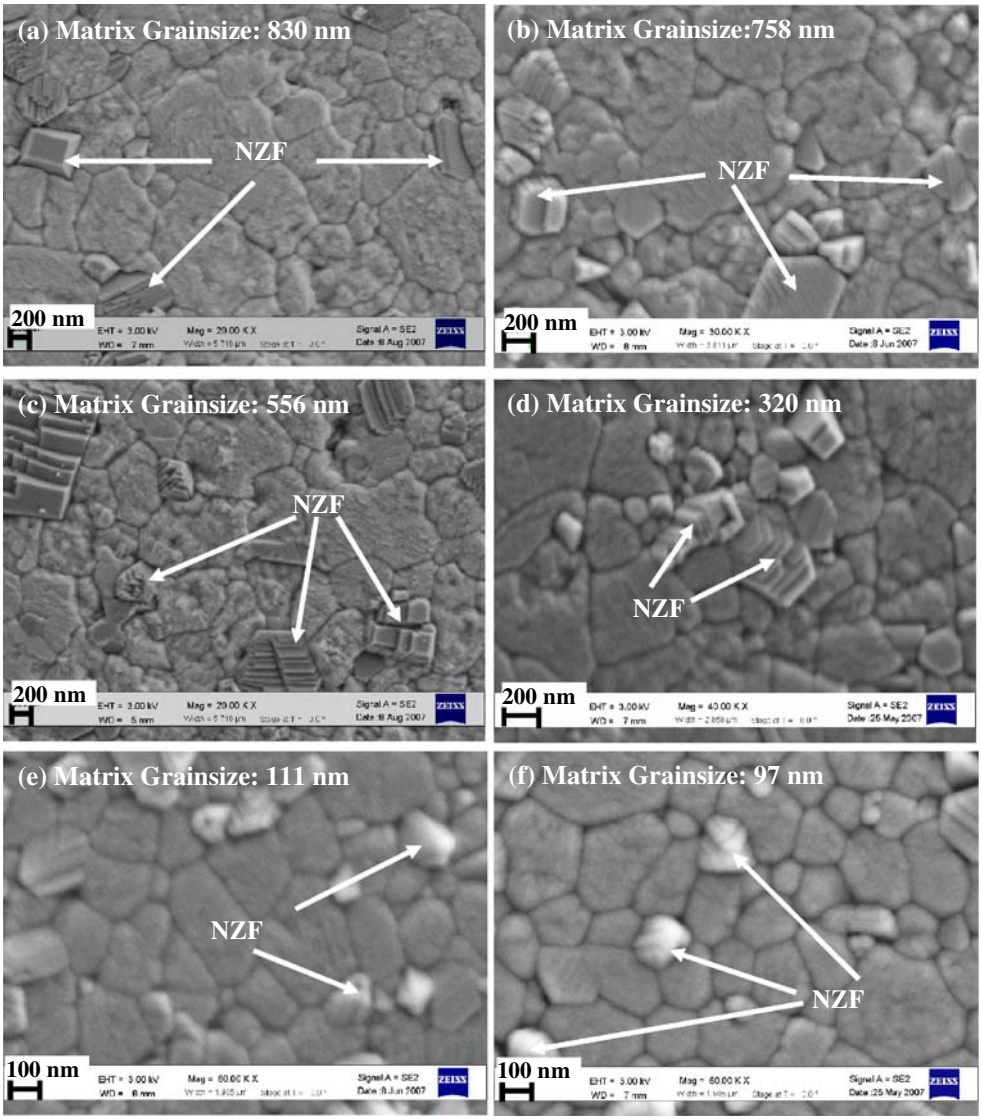


**Fig. 3** Microstructures of ME composites with varying grain size (**a**) 830 nm, (**b**) 758 nm, (**c**) 556 nm, (**d**) 320 nm, (**e**) 111 nm, and (**f**) 97 nm

reaches about 98%. The densification decreases to 93% as the grain size increases to 750 nm. Figure 4b shows the variation of resistivity as a function of the grain size. For a small grain size of 97 nm the resistivity exhibited a magnitude of $1.23 \times 10^{10}$ Ω-cm, whereas for the large grain size of 600 nm the value increased to $7.15 \times 10^{10}$ Ω-cm. The increase in resistivity at higher grain size indicates that ferrite grain size and distribution is affected by growth of piezoelectric phase. Figure 5 shows the sintered composite XRD patterns for different grain sizes. Major peaks of perovskite (marked as P) and spinel (marked as S) were observed with no trace of any other intermediate phase. The peak width (FWHM) also follows the same trend; with increasing grainsize from 97 to 758 nm, FWHM decreases from 0.411 to 0.245 deg.

Figure 6a and b shows the variation of longitudinal piezoelectric strain constant ($d_{33}$), dielectric constant ($\varepsilon_r/\varepsilon_o$), and longitudinal piezoelectric voltage constant ($g_{33}$) with matrix (PZT) grain size. It can be noticed in this figure that there is a critical grain size below which the piezoelectric properties drop rapidly. The critical grain size is in the range of 100–150 nm. Above 200 nm the piezoelectric properties increases slowly and saturates at 600 nm. The magnitude of $d_{33}$, $\varepsilon_r/\varepsilon_o$, and $g_{33}$ for ME composite with grain size of 97 nm were 44 pC/N, 659 and $7.5 \times 10^{-3}$ V-m/N. This magnitude increases rapidly to 65 pC/N, 746 and $9.9 \times 10^{-3}$ V-m/N at grain size of 215 nm. Above 600 nm the piezoelectric and dielectric properties saturate at the magnitude of 72 pC/N, 781 and $10.4 \times 10^{-3}$ V-m/N. There is a slight drop in piezoelectric and dielectric constant around 500–600 nm grain size, which can be related to the changes in domain structure (90° domains) [12, 23]. Arlt has described the transition region where complex banded domain structure changes to lamella structure [24]. The

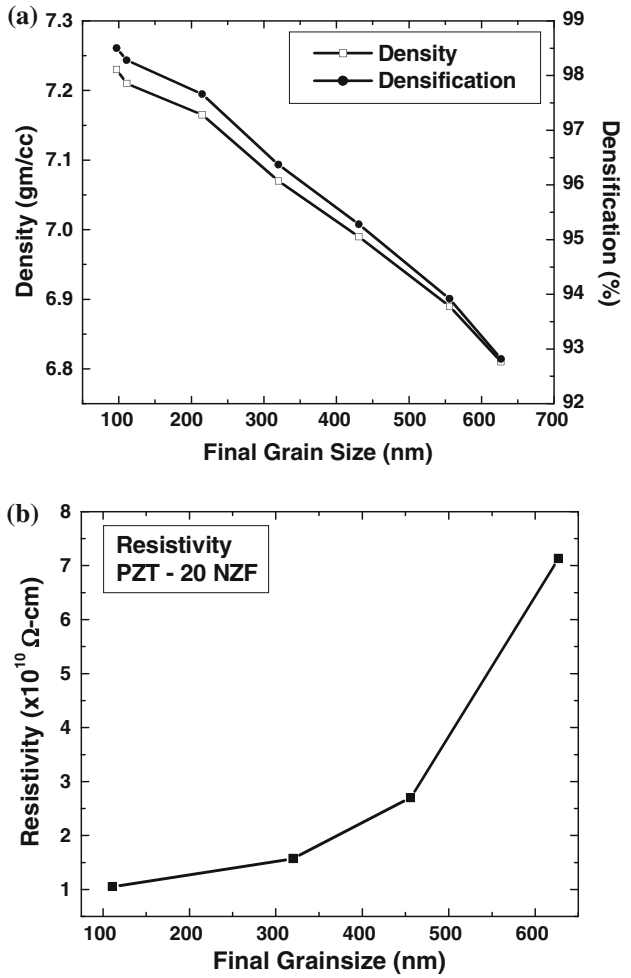


**Fig. 4** Variation of physical property with grain size (**a**) Density and densification, and (**b**) resistivity

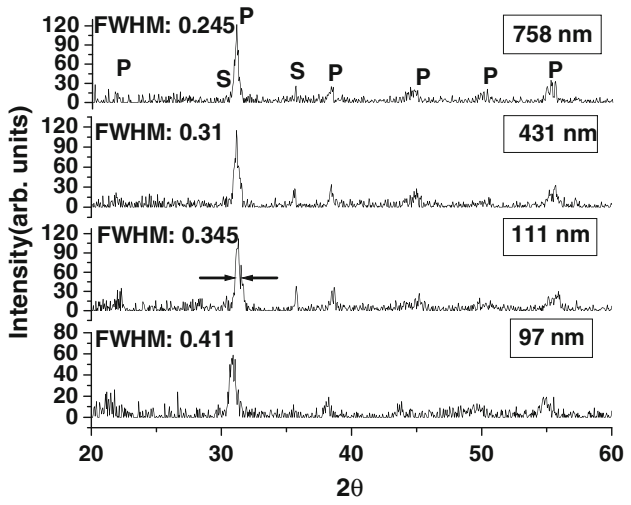


**Fig. 5** XRD patterns of the sintered composite showing perovskite (P) and spinel (S) peaks

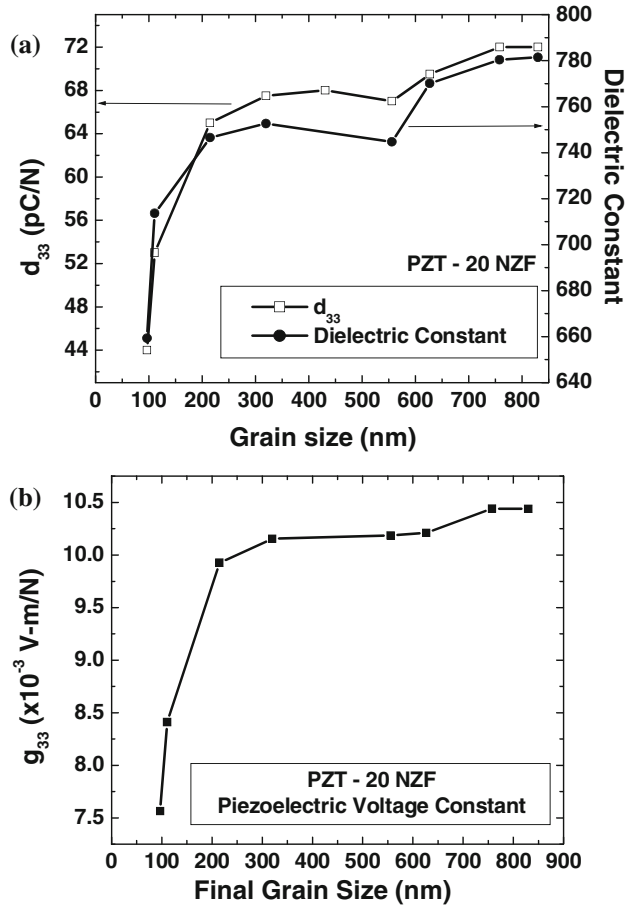


**Fig. 6** Piezoelectric properties as a function of grain size (**a**) Longitudinal piezoelectric and dielectric constant and (**b**) piezoelectric voltage constant

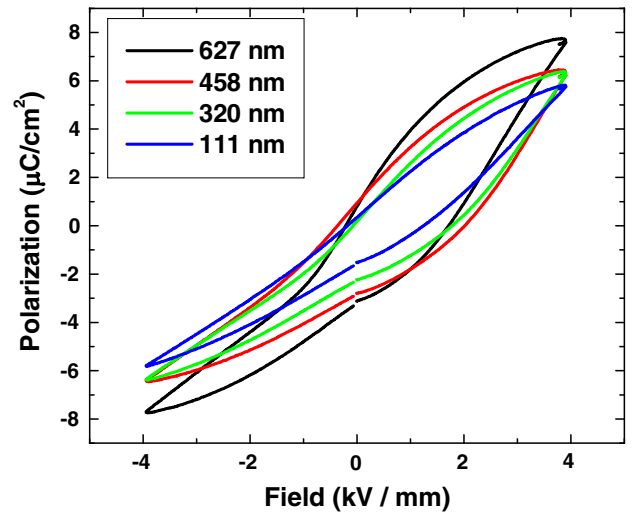


**Fig. 7** Polarization vs. electric field loop as a function of grainsize

increase in the piezoelectric and dielectric properties as the grain size increases from 100 to 200 nm can be explained in terms of domain wall motion. For larger grains, where the

size of the domain is smaller than the size of the grains, the movement of the domain walls is easier. On the other hand, in small grains the movement of domain walls is restricted by the grain boundary. As a result during poling the domain switching will be difficult which reduces the piezoelectric properties [13]. The decrease in the magnitude of the piezoelectric constant (72 pC/N for 600 nm grain size) as compared to the original PZT composition (~220 pC/N) does indicate there is interdiffusion of ions. However, we have not studied the nature of diffusing species and diffusion distances.

Figure 7 shows the polarization versus electric field loop for PZT–20 NZF for four different matrix (PZT) grain sizes. It was found that as the grain size increases the squareness of the loop increases. Saturation polarization ($P_s$) and coercive field ($E_c$) increases with the increase in grain size. $P_s$ and $E_c$ values of 7.68 μC/cm$^2$ and 1.7 kV/mm were measured at 627 nm grain size. These values were found to be 5.79 μC/cm$^2$ and 1.2 kV/mm for 111 nm grain size. The low values of $P_s$ and coercivity at smaller grain sizes can be explained in terms of nucleation sites density. The number of nucleation sites for new domains are more in smaller grain size during polarization switching thus resulting in smaller $E_c$ [14]. Similar behavior was observed in the dielectric constant versus temperature plot as shown in Fig. 8. It was found that as the grain size increases the dielectric constant increase and Curie temperature slightly increases. From the dielectric data at 100 kHz it can be seen

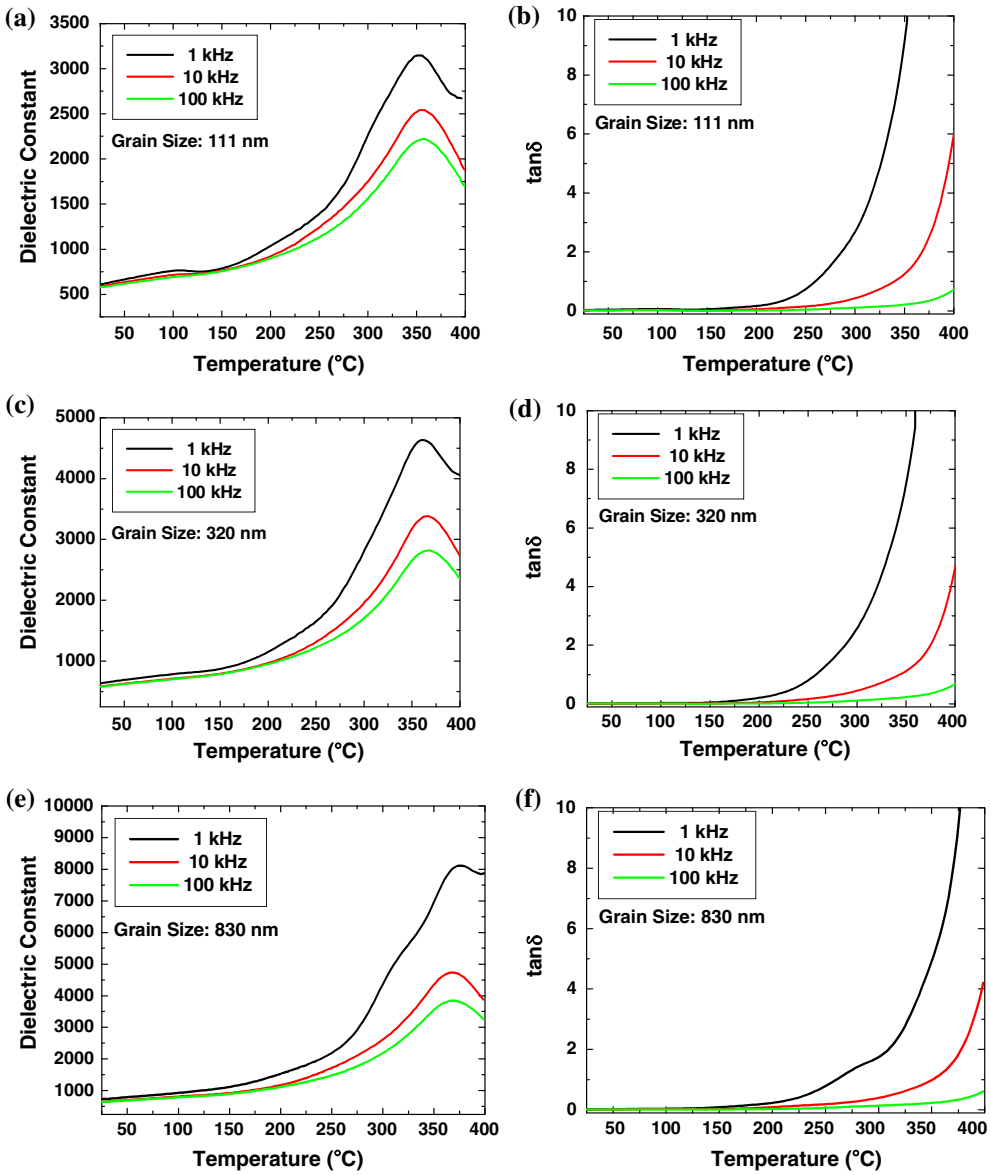


**Fig. 8** Dielectric properties as a function of temperature (**a**) dielectric constant for 111 nm, (**b**) loss factor for 111 nm, (**c**) dielectric constant for 320 nm, (**d**) loss factor for 320 nm, (**e**) dielectric constant for 830 nm, and (**f**) loss factor for 830 nm

that at grain size of 111 nm the dielectric maximum occurs at 355.8 °C while at grain size of 830 nm the dielectric maximum occurs at 368.5 °C. Figure 8b, d, and f shows the variation of dielectric loss factor (tan $\delta$) as a function of temperature. The loss factor increases rapidly at high temperatures indicating the space charge conduction and is significantly smaller at high frequency of 100 kHz. Space charge conduction is related to the transport of defects such as oxygen vacancies to the dielectric–electrode interface [25, 26]. In general, for smaller grain size the loss factor is lower because the grain boundary acts as pining site for the domain wall movement [13–15]. From the data in Fig. 8, the loss factor at 100 kHz and 30 °C was found to be 0.0113 for 111 nm grain size while 0.00696 for 830 nm grain size. At the temperature of dielectric maximum and 100 kHz frequency the loss factor for 111 nm grain size was found to be 0.232 while that for 830 nm it was found to be 0.297.

The magnetic properties of the composites with different matrix grain sizes were found to be in the same range as shown in Table 1. The saturation magnetization varied between 10.3 and 10.8 emu/gm and the remnant magnetization varied between 0.71 and 0.88 emu/gm. The $E_c$ for all the composites was between 62.2 and 75.1 Oe. The data in Table 1 indicates that the variation in the ME property of these composite will depend upon the piezoelectric properties of the matrix. Figure 9a shows the variation of the ME voltage coefficient as a function of the grain size. As the grain size decreases, ME voltage coefficient drops and shows similar trend as that of piezoelectric property. Above 200 nm grain size, the ME voltage coefficient increases and it saturates above 600 nm as shown in Fig. 9b. For the grain size of 97 and 830 nm the ME voltage coefficient was found to be as 54.4 and 157.5 mV/cm.Oe, respectively.

The results of this study demonstrate that grain size can be used to modulate the magnitude of piezoelectric and dielectric constant which effect the magnitude of the ME coefficient. It is well known that large magnitude of ME susceptibility requires high dielectric permittivity of the piezoelectric phase and high magnetic permeability of magnetostrictive phase [27, 28]. Zubkov has also proposed the following expression for the ME voltage coefficient ($\alpha_E$) [29]:

$$\alpha_E = (\mathrm{dE/dH})_{\mathrm{comp}} = (\mathrm{dS/dH})_{\mathrm{comp}}(\mathrm{dE/dS})_{\mathrm{comp}} = m_v(\mathrm{dS/dH})_{\mathrm{ferrite}}(1 - m_v)(\mathrm{dE/dS})_{\mathrm{piezoelectric}} \quad (1)$$

where $m_v$ is the volume fraction of ferrite, (dE/dS) is the inverse of change in strain per unit electric field, and (dS/dH) is the change in strain per unit magnetic field. Since, dE = g.dX and dS = dX/C, where X is the stress, S is strain, g is piezoelectric voltage constant, and C is the stiffness, Eq. 1 can be written as:

$$\alpha_E = m_v(\mathrm{dS/dH})_{\mathrm{ferrite}}(1 - m_v)\left(g_{ij}C_{ij}\right)_{\mathrm{piezoelectric}} \quad (2)$$

Assuming the deformation is occurring along the thickness direction and electric field is measured along the same direction, Eq. 2 can be approximated as:

**Table 1** Magnetic properties of the composite as a function of average matrix grain size

| Grain size (nm) | Saturation magnetization (emu/gm) | Remnant magnetization (emu/gm) | Coercive field (Oe) |
|---|---|---|---|
| 97 | 10.8 | 0.84 | 75.1 |
| 215 | 10.8 | 0.75 | 66.9 |
| 320 | 10.5 | 0.76 | 69.6 |
| 431 | 10.4 | 0.72 | 66.1 |
| 556 | 10.7 | 0.88 | 67.9 |
| 620 | 10.4 | 0.79 | 67.3 |
| 758 | 10.6 | 0.87 | 73.9 |
| 830 | 10.3 | 0.71 | 62.2 |

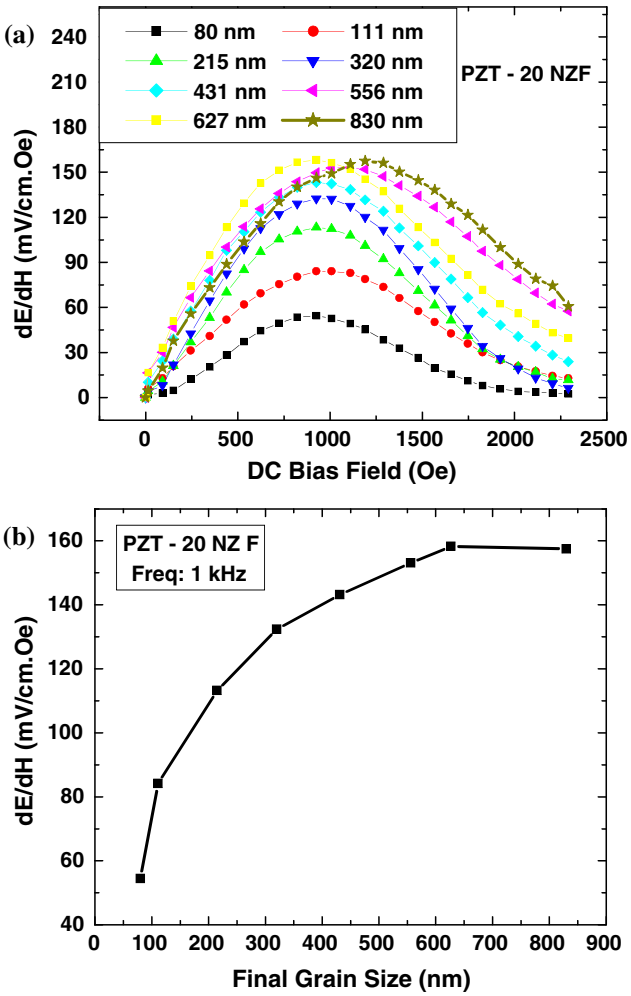


**Fig. 9** Magnetoelectric coefficient as a function of (**a**) DC bias field and (**b**) grain size

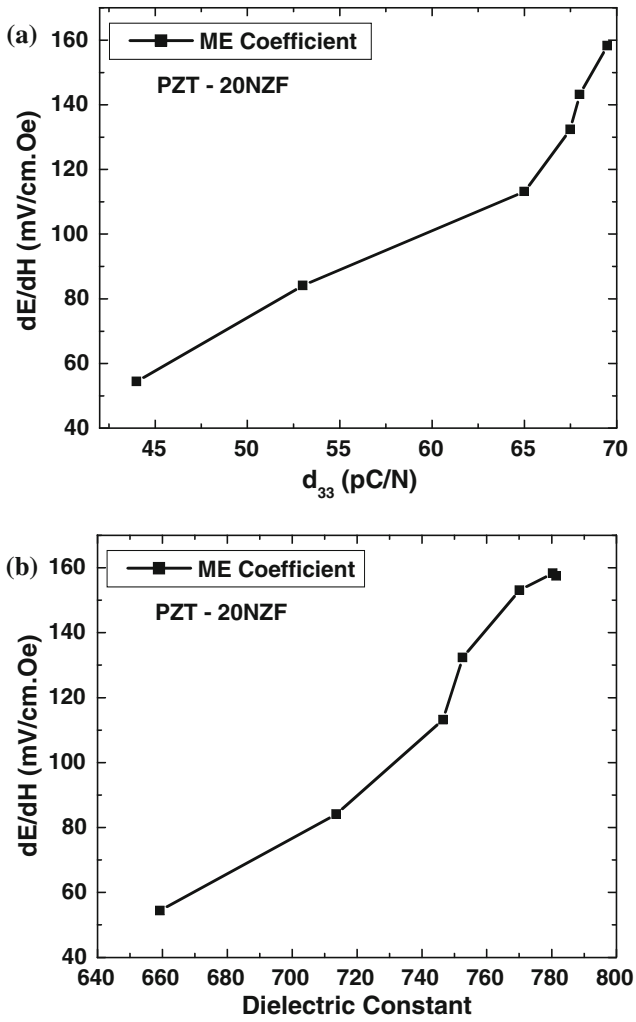


**Fig. 10** Magnetoelectric coefficient as a function of (**a**) piezoelectric strain constant and (**b**) dielectric constant

$$\alpha_E = m_v(\mathrm{dS/dH})_{\mathrm{ferrite}}(1 - m_v)(g_{33}C_{33})_{\mathrm{piezoelectric}} \quad (3)$$

Figure 10a and b shows the variation of ME coefficient with piezoelectric constant and dielectric constant. It was found that as the piezoelectric and dielectric constant increases the ME coefficient increases. At larger grain size (above 600 nm) where dielectric constant saturates to a value of 780, ME coefficient was also found to be saturated to a value of 155 mV/cm.Oe. Using Eq. 3, the magnitude of ME voltage coefficient can be approximated as following. The magnitude of the (dS/dH) for common ferrite materials is of the order of $1 \times 10^{-9}$ m/A (=$79.577 \times 10^{-9}$ $\mathrm{Oe}^{-1}$), [30] $m_v = 0.2$, and $C_{33} \sim 11 \times 10^{10}$ $\mathrm{N/m}^2$ [31]. Substituting these values in Eq. 3, the ME coefficient can be expressed in terms of piezoelectric voltage coefficient as:

$$\alpha_E = 1400.5(g_{33})_{\mathrm{piezoelectric}} \quad (4)$$

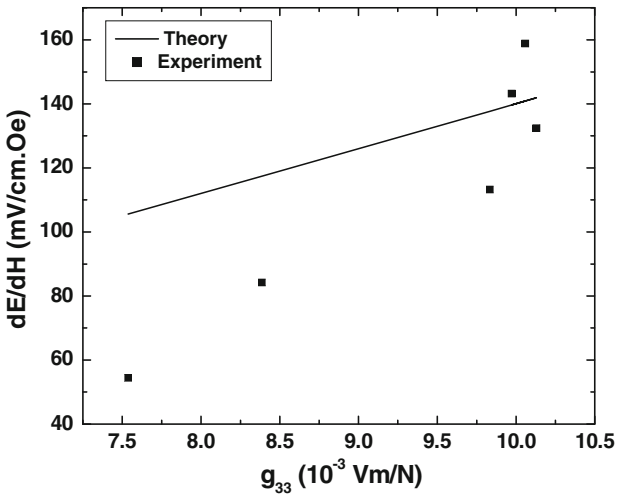


**Fig. 11** Comparison of the measured ME coefficient with that predicted from theory

Figure 11 compares the plot of the ME voltage coefficient calculated using the data from Fig. 10 and Eq. 4 with that of experimental measurement. At higher grain sizes or higher magnitude of $g_{33}$, the magnitude of ME voltage coefficient shows similar trend as that predicted by Eq. 4. However, at lower grain sizes the magnitude of the measured ME coefficient is lower than that predicted by Eq. 4. The reason could be that the derivation of Eq. 4 does not take into account any microstructure variable such domain size and grain boundary defect density. In general, the grain size is related to domain size through the expression [32]:

$$\text{Domain size} \propto (\text{Grain size})^m$$

where $m > ½$ for grain size <1 μm. Thus, with increasing grain size the contribution from extrinsic effects, i.e., domain wall motion will increase which could provide some explanation for the enhancement of the ME coefficient. For the calculation of Fig. 11, the elastic stiffness was taken as a constant. However, it is known that elastic properties vary with the grain size and it should be accommodated in the model. Further, it was assumed in the derivation that elastic modulus of the ferrite and piezoelectric are equal and there is perfect coupling of strain. This may not hold true if the defects present at the interfaces which produces elastic softening.

## Conclusion

This study investigates the effect of grain size on the ME coefficient of PZT–20 NZF particulate composites. It was found that grain size has significant effect on the

piezoelectric, ferroelectric, and dielectric properties of the composite and hence influences the ME property. Samples having grain size of around 100 nm show small magnitude of ME Coefficient (54.4 mV/cm.Oe) while those with grain size of 600 nm exhibit a value of 155 mV/cm.Oe.

**Acknowledgement** The authors are grateful to Office of Basic Energy Science, Department of Energy for supporting this research.

## References

1. Suchetelene JV (1972) Philips Res Rep 27:28
2. Weng L, Fu Y, Song S, Tang J, Li J (2007) Scripta Mater 56:465
3. Ren SQ, Weng LQ, Song SH, Li F, Wan JG, Zeng M (2005) J Mater Sci 40(16):4375. doi:10.1007/s10853-005-1057-1
4. Wu D, Gong W, Deng H, Li M (2007) J Phys D: Appl Phys 40:5002
5. Srinivasan G, DeVreugd CP, Flattery CS, Laletsin VM, Paddubnaya N (2004) Appl Phys Lett 85(13):2550
6. Van Run AMJG, Terrell DR, Scholing JH (1974) J Mater Sci 9:1710. doi:10.1007/BF00540771
7. Lupeiko TG, Lisnevskaya IV, Chkheidze MD, Zvyagintsev BI (1995) Inorg Mater 31:1139
8. Lupeiko TG, Lopatina IB, Lopatin SS, Getman IP (1991) Neorg Mater 27(11):2394
9. Bokhan YI, Laletin VM (1996) Inorg Mater 32(5):634
10. Lupeiko TG, Lopatin SS, Lisnevskaya IV, Zvyagintsev BI (1994) Inorg Mater 30:1353
11. Ryu J, Carazo AV, Uchino K, Kim HE (2001) J Electroceram 7:17
12. Kang BS, Choi DG, Choi SK (1998) K Kor Phys Soc 32:S232
13. Martirena HT, Burfoot JC (1974) J Phys C: Solid State Phys 7:3182
14. Choudhury S, Li YL, Krill C, Chen LQ (2007) Act Mater 55:1415
15. Duiker HM, Beale PL (1990) Phys Rev B 41(1):490
16. Sundar V, Kim N, Randall CA, Yimnirun R, Newnham RE (1996) The Effect of Doping and Grain Size On Electrostriction in $Pb(Zr_{0.52}Ti_{0.48})0_3$. Proceedings of the 10th IEEE International Symposium on Application of Ferroelectrics, p 935
17. Lu CJ, Ren SB, Shen HM, Liu JS, Wang YN (1996) J Phys Condens Matter 8:8011
18. Sakaki C, Newalkar BL, Komerneni S, Uchino K (2001) Jpn J Appl Phys 40:6907
19. Randall CA, Kim N, Kucera JP, Cao WW, Shrout TR (1998) J Am Ceram Soc 81:677
20. Jin BM, Kim J, Kim SC (1997) Appl Phys A: Mater Sci Proc 65:53
21. Shaw TM, Mckinstry ST, Mcintyre PC (2000) Ann Rev Mater Sci 30:263
22. Zhao Z, Buscaglia V, Viviani M, Buscaglia MT, Mitoseriu L, Testino A et al. (2004) Phys Rev B 70:024107
23. Uchino K (1997) Piezoelectric actuators and ultrasonic motors. Kluwer Academic Publishers, USA, p 61
24. Arlt G (1990) J Mater Sci 25:2655
25. Zhang S, Priya S, Shrout TR, Randall CA (2003) J Appl Phys 93:2880
26. Chen Y-H, Uchino K, Viehland D (2001) J Appl Phys 89:3928
27. Dong S, Zhai J, Li J, Viehland D (2006) Appl Phys Lett 89:252904
28. Islam RA, Viehland D, Priya S (2008) J Mater Sci Lett 43(4):1497
29. Zubkov AS (1978) Elektrichestvo 10:77
30. Jiles DC (2003) Acta Mater 51:5907
31. Gautschi G (2002) Piezoelectric sensorics. Springer, NY
32. Cao W, Randall CA (1996) J Phys Chem Solids 57:1499